Revision 1

Terrywallaceite, $AgPb(Sb,Bi)_3S_6$, isotypic with gustavite, a new mineral from Mina Herminia, Julcani Mining District, Huancavelica, Peru

Hexiong Yang[1*], Robert T. Downs[1], Stanley H. Evans[1], and William W. Pinch[2]

[1]Department of Geosciences, University of Arizona, Tucson, Arizona 85721-0077, U.S.A.

[2]19 Stonebridge Lane, Pittsford, New York 14534-1800, U.S.A.

*Corresponding author: hyang@u.arizona.edu

Abstract

A new mineral species, terrywallaceite, ideally $AgPb(Sb,Bi)_3S_6$, has been found in Mina Herminia, Julcani Mining District, Huancavelica, Peru. It is associated with tetrahedrite, gustavite, barite, and pyrite. Terrywallaceite crystals are lath-shaped, metallic-black, with striations parallel to the elongated direction (the *c* axis). The mineral is opaque with black streak and metallic luster. It is brittle and has a Mohs hardness of ~4; cleavage is good on {010} and no parting was observed. Twinning is pervasive on (100). The calculated density is 6.005 g/cm^3. Optically, terrywallaceite is greyish white in polished thin section, with weak bireflectance, weak pleochroism (white to pale grey), and weak anisotropy (grey with bluish tint to bluish black in air). An electron microprobe analysis yielded an empirical formula, based on 6 (S + As) apfu, $Ag_{1.02}Pb_{0.87}(Sb_{1.53}Bi_{1.47})_{\Sigma=3.00}(S_{5.94}As_{0.06})_{\Sigma=6.00}$.

Terrywallaceite is a member of the lillianite group and isostructural with $P2_1/c$ gustavite. Its unit-cell parameters are a = 6.9764(4), b = 19.3507(10), c = 8.3870(4) Å, β = 107.519(2)°, and V = 1079.7(1) Å^3. The structure of terrywallaceite contains six symmetrically-nonequivalent S sites and five cation sites [Ag, Pb, M1 (= 0.82Bi + 0.18Sb), M2 (= 0.60Bi + 0.40Sb), and M3 (= 0.95Sb + 0.05Bi)]. The pronounced

preference of Sb for the M3 site over M2 and M1 in terrywallaceite is consistent with the site occupancy data reported for Sb-bearing gustavite, and suggests an alternative ideal formula for terrywallaceite of $AgPb(Sb,Bi)(Bi,Sb)_2S_6$, instead of $AgPb(Sb,Bi)_3S_6$.

***Key words*:** Terrywallaceite, gustavite, $AgPb(Sb,Bi)_3S_6$, sulfosalt, crystal structure, X-ray diffraction

Introduction

A new sulfosalt mineral species, terrywallaceite, ideally $AgPb(Sb,Bi)_3S_6$, has been found in Mina Herminia, Julcani Mining District, Huancavelica, Peru. The mineral is named after Dr. Terry C. Wallace, Jr., a former professor of geosciences and mineral museum curator specializing in silver minerals at the University of Arizona for over 20 years. Dr. Wallace joined Los Alamos National Laboratory (LANL) in 2003 and now is the Principal Associate Director for science, technology, engineering, and educational activities at LANL. The new mineral and its name have been approved by the Commission on New Minerals, Nomenclature, and Classification (CNMNC) of the International Mineralogical Association (IMA 2011-017). Part of the cotype sample has been deposited at the University of Arizona Mineral Museum (Catalogue # 19034) and the RRUFF Project (deposition # R100007: http://rruff.info/terrywallaceite).

Terrywallaceite is a member of the lillianite ($Pb_3Bi_2S_6$) group of Ag-Pb-Bi-Sb sulfosalt minerals (Moëlo et al. 2008). The structural and chemical features of the lillianite homologues have been described in length by Makovicky and Karup-Møller (1977a, 1977b), and Makovicky (2006). This paper describes the physical and chemical properties of terrywallaceite and its crystal structure determined from single-crystal X-ray diffraction data.

Sample Description and Experimental Methods

Occurrence, physical and chemical properties

Terrywallaceite was found on a rock sample collected from Level 390, Vein 14, Mina Herminia, Julcani Mining District, Huancavelica, about 300 km southeast of Lima, Peru. Associated minerals include tetrahedrite $Cu_{12}Sb_4S_{13}$, gustavite $AgPbBi_3S_6$, barite $BaSO_4$, and pyrite FeS_2. The mineralization at the Julcani District is genetically related to a geologically brief pulse of late Miocene (~10 m.y.) calc-alkalic magmatic activity (Goodell and Petersen 1974; Petersen et al. 1977; Lueth et al. 1990; Sack and Goodell 2002, and references therein). Hydrothermal alteration and mineralization are believed to have taken place concurrently with the intrusion of late-stage volcanic domes and dikes.

Terrywallaceite crystals are lath-shaped, black, with striations parallel to the elongated direction (the **c** axis) and up to 0.5 mm long (Figs. 1 and 2). The mineral is opaque with black streak and metallic luster. It is brittle and has a Mohs hardness of ~4; cleavage is good on {010} and no parting was observed. Twinning is pervasive on (100). The calculated density is 6.005 g/cm^3. Optically, terrywallaceite is greyish white in polished thin section, with weak bireflectance, weak pleochroism (white to pale grey), and weak anisotropy (grey with bluish tint to bluish black in air). The reflectance values of terrywallaceite (Table 1) were measured using a Zeiss MPM800 microscope-spectrophotometer system relative to the spectra from a WTiC reflectance standard (Zeiss 314).

The chemical composition of terrywallaceite was determined using a CAMECA SX-100 electron microprobe (20 kV, 20 nA, 20 μm beam diameter). The standards included galena (S, Pb), $AgBiS_3$ (Ag, Bi), NiAs (As), and stibnite (Sb), yielding an average composition (15 points, wt.%) of S 19.32(29), Bi 31.10(53), Sb 18.94(22), As 0.45(3), Ag 11.19(26), and Pb 18.22(49), and total = 99.24(69). The resultant chemical formula, calculated on the basis of 6 (S + As) atoms per formula, is

$Ag_{1.02}Pb_{0.87}(Sb_{1.53}Bi_{1.47})_{\Sigma=3.00}(S_{5.94}As_{0.06})_{\Sigma=6.00}$, which can be simplified to $AgPb(Sb,Bi)_3S_6$.

X-ray crystallography

Both powder and single-crystal X-ray diffraction data of terrywallaceite were collected on a Bruker X8 APEX2 CCD X-ray diffractometer equipped with graphite-monochromatized MoK_α radiation. Listed in Table 2 are the measured powder X-ray diffraction data, along with those calculated from the determined structure using the program XPOW (Downs et al. 1993).

Before the single-crystal X-ray diffraction data collection, several crystals of terrywallaceite were examined and they all appeared to be twinned on (100), with the twin law (1 0 0.5, 0 -1 0, 0 0 -1) (Fig. 2). The X-ray intensity data were collected from a nearly equi-dimensional twinned crystal (0.05 x 0.05 x 0.06 mm) with frame widths of 0.5° in ω and 30 s counting time per frame. All reflections were indexed on the basis of a monoclinic unit-cell (Table 3) and processed with the software TWINABS (Sheldrick 2007). The systematic absences of reflections indicate the unique space group $P2_1/c$ (#14). The crystal structure was solved and refined using SHELX97 (Sheldrick 2008). The positions of all atoms were refined with anisotropic displacement parameters. The labeling scheme of the atomic sites follows that adopted by Makovicky and Topa (2011). During the structure refinements, the small amount of As detected from the chemical analysis was ignored; all S, Ag, and Pb sites were assumed to be fully occupied by S, Ag, and Pb, respectively. The total amounts of Sb and Bi were constrained to those determined from electron microprobe analysis, but their ratios at the three individual sites (M1, M2, and M3) were allowed to vary. Final coordinates and displacement parameters of atoms are listed in Table 4, and selected bond-distances in Table 5.

Discussion

Terrywallaceite is isostructural with $P2_1/c$ gustavite, $AgPbBi_3S_6$ (Pažout and Dušek 2009; Makovicky and Topa 2011), an endmember of the gustavite-lillianite solid solution series ($Ag_xPb_{3-2x}Bi_{2+x}S_6$). Its structure contains six symmetrically-nonequivalent S sites and five cation sites (Ag, Pb, M1, M2, and M3) (Table 4). Most remarkably, the M1, M2, and M3 sites are occupied by (Bi + Sb) with different ratios: While the M1 (= 0.82Bi + 0.18Sb) and M2 (= 0.60Bi + 0.40Sb) sites are preferentially occupied by Bi, the M3 site is predominately filled with Sb (0.95Sb + 0.05Bi). Viewed along ***c****, the structure of terrywallaceite consists of alternating slabs of PbS archetype cut parallel to $(311)_{PbS}$ and each slab has $N = 4$, the number of octahedra running diagonally across an individual slab, which are Ag, M2, M3, and M1 (Fig. 4) (Makovicky and Karup-Moller 1977a, 1977b; Makovicky 2006). The octahedral slabs are separated by rods of Pb atoms in a bicapped trigonal prismatic coordination. The four distinct octahedra in a slab are all appreciably distorted, with Ag in a 4+2 coordination (four short bonds and two long ones), and M1, M2, and M3 in the 3+3 coordination (Table 5). For comparison, listed in Table 5 are also selected bond distances for gustavite examined by Pažout and Dušek (2009) and Makovicky and Topa (2011).

Natural gustavite samples generally contain some amounts of Sb substituting for Bi, with the Sb/(Sb+Bi) ratios ranging between 0 and 31% (see Pažout et al. 2001; Pažout and Dušek 2009 and references therein). The discovery of terrywallaceite extends the Sb/(Sb+Bi) ratio in the gustavite-type structure over 50%. However, there is apparently no complete solid solution between $AgPbBi_3S_6$ and $AgPbSb_3S_6$, because the latter crystallizes in the $Pn2_1a$ andorite VI structure (Sawada et al. 1987), instead of the $P2_1/c$ gustavite-type structure. Accordingly, based on the chemical analysis, we propose the chemical formula for terrywallaceite as $AgPb(Sb,Bi)_3S_6$, rather than $AgPbSb_3S_6$. However, the exact phase boundary between terrywallaceite and andorite VI in terms of the Sb/Bi ratio is still unclear at present. The most Bi-rich andorite found thus far has

Sb/(Sb+Bi) = 0.77 (Pažout and Dušek 2010). Therefore, the phase boundary between terrywallaceite and andorite VI should fall between Sb/(Sb+Bi) = 0.51 and 0.77.

Interestingly, compounds with the gustavite chemistry display either $P2_1/c$ (Pažout and Dušek 2009; Makovicky and Topa 2011) or *Cmcm* symmetry (Bente et al., 1993). Similarly, an unnamed mineral, nominally with the terrywallaceite chemistry [$Ag_{0.71}Pb_{1.52}(Bi_{1.32}Sb_{1.45})_{2.77}S_6$, Sb/(Sb+Bi) = 52.3%], was reported to also have an orthorhombic *Cmcm* symmetry (Pažout and Dušek 2010). Nevertheless, it should be noted that the Pb content in the orthorhombic phase studied by Pažout and Dušek (2010) is significantly greater than 1.0, making it questionable to include this phase in the $AgPbBi_3S_6$-$AgPbSb_3S_6$ system.

Analogous to Sb-bearing gustavite (Pažout and Dušek 2009; Makovicky and Topa 2011), terrywallaceite also displays a marked preference of Sb for the M3 site over M2 and M1. In fact, it appears that, as illustrated in Figure 5, the occupancy of Sb at the M3 site will exceed that of Bi when the Sb/(Sb+Bi) ratio for the whole $AgPb(Bi,Sb)_3S_6$ solid solution is only about 25%. This, then, calls into question whether it would be more appropriate and reasonable to express the structural formula of terrywallaceite as $AgPb(Sb,Bi)(Bi,Sb)_2S_6$, instead of $AgPb(Sb,Bi)_3S_6$. If so, the phase boundary between gustavite and terrywallaceite should be at Sb/(Sb+Bi) ≈ 25%, rather than 50%. This argument would also put the Sb-rich gustavite, $Ag_{1.08}Pb_{0.84}(Bi_{2.11}Sb_{0.96})(S_{5.93}Se_{0.01})$, investigated by Pažout and Dušek (2009) into the terrywallaceite compositional field, in which the M3 site is occupied by (0.65Sb + 0.35 Bi).

Acknowledgements

This study was funded by the Science Foundation Arizona.

References Cited

Bente, K., Engel, M., and Steins, M. (1993) Crystal structure of lead silver tribismuth sulfide: $PbAgBi_3S_6$. Zeitschrift für Kristallographie, 205, 327-328.

Downs, R.T., Bartelmehs, K.L., Gibbs, G.V. and Boisen, M.B., Jr. (1993) Interactive software for calculating and displaying X-ray or neutron powder diffractometer patterns of crystalline materials. American Mineralogist, 78, 1104-1107.

Goodell, P.C. and Petersen, U. (1974) Julcani mining district, Peru: A study of metal ratios. Economical Geology, 69, 347-361.

Lueth, V.W., Goodell, P.C., and Pingitore, N.E. (1990) Encoding the evolution of an ore system in bismuthinite– stibnite composit ions. Economic Geology, 85, 1462-1472.

Makovicky, E. (2006) Crystal structures of sulfides and other chalcogenides. Reviews in Mineralogy and Geochemistry, 61, 7–125.

Makovicky, E. & Karup-Møller, S. (1977a): Chemistry and crystallography of the lillianite homologous series. I. General properties and definitions. Neues Jahrbuch für Mineralogie, Abhandlungen, 130, 264–287.

—, — (1977b): Chemistry and crystallography of the lillianite homologous series. II. Definition of new minerals: eskimoite, vikingite, ourayite, and treasurite. Redefinition of schirmerite and new data on the lillianite-gustavite solid-solution series. Neues Jahrbuch für Mineralogie, Abhandlungen, 131, 264-287.

Makovicky, E. and Topa, D. (2011) The crystal structure of gustavite, $PbAgBi_3S_6$. Analysis of twinning and polytypism using the OD approach, European Journal of Mineralogy, 23, 537-550.

Moëlo, Y., Makovicky, E., Mozgova, N.N., Jambor, J.L., Cook, N., Pring, A., Paar, W., Nickel, E.H., Graeser, S., Kapup-Møller, S., Balic-Zunic, T., Mumme, W.G., Vurro, F., Topa, D., Bindi, L., Bente, K. & Shimizu, M. (2008) Sulfosalt systematics: a review. Report of the sulfosalt sub-committee of the IMA Commission on Ore Mineralogy. European Journal of Mineralogy, 20, 7-46.

Pažout, R., Ondruš, P., and Šrein, V. (2001) Gustavite with variable Bi/Sb ratio from Kutná Hora deposit, Czech Republic, a new occurrence. Neues Jahrbuch für Mineralogie, Monatshefte, 2001, 157-168.

Pažout, R. and Dušek, M. (2009) Natural monoclinic $AgPb(Bi_2Sb)_3S_6$, an Sb-rich gustavite. Acta Crystallographica, C65, i77-i80.

Pažout, R. and Dušek, M. (2010) Crystal structure of natural orhtorhombic $Ag_{0.71}Pb_{1.52}Bi_{1.32}Sb_{1.45}S_6$, a lillianite homologue with N=4; comparison with gustavite. European Journal of Mineralogy, 22, 741-750.

Petersen, U., Noble, D.C., Arenas, M.J., and Goodell, P.C. (1977) Geology of the Julcani mining district, Peru. Economical Geology, 72, 931-949.

Sack, R.O. and Goodell, P.C. (2002) Retrograde reactions involving galena and Ag-sulphosalts in a zoned ore deposit, Julcani, Peru. Mineralogical Magazine, 66, 1043-1062.

Sawada, H., Kawada, I., Hellner, E., and Tokonami, M. (1987) The crystal structure of senandorite (andorite VI): $PbAgSb_3S_6$. Zeitschrift für Kristallographie, 180, 141-150.

Sheldrick, G. M. (2007) TWINABS. University of Göttingen, Germany.

_____ (2008) A short history of *SHELX*. Acta Crystallographica, A64, 112-122.

List of Tables

List of Figure Captions


R100007
1 cm

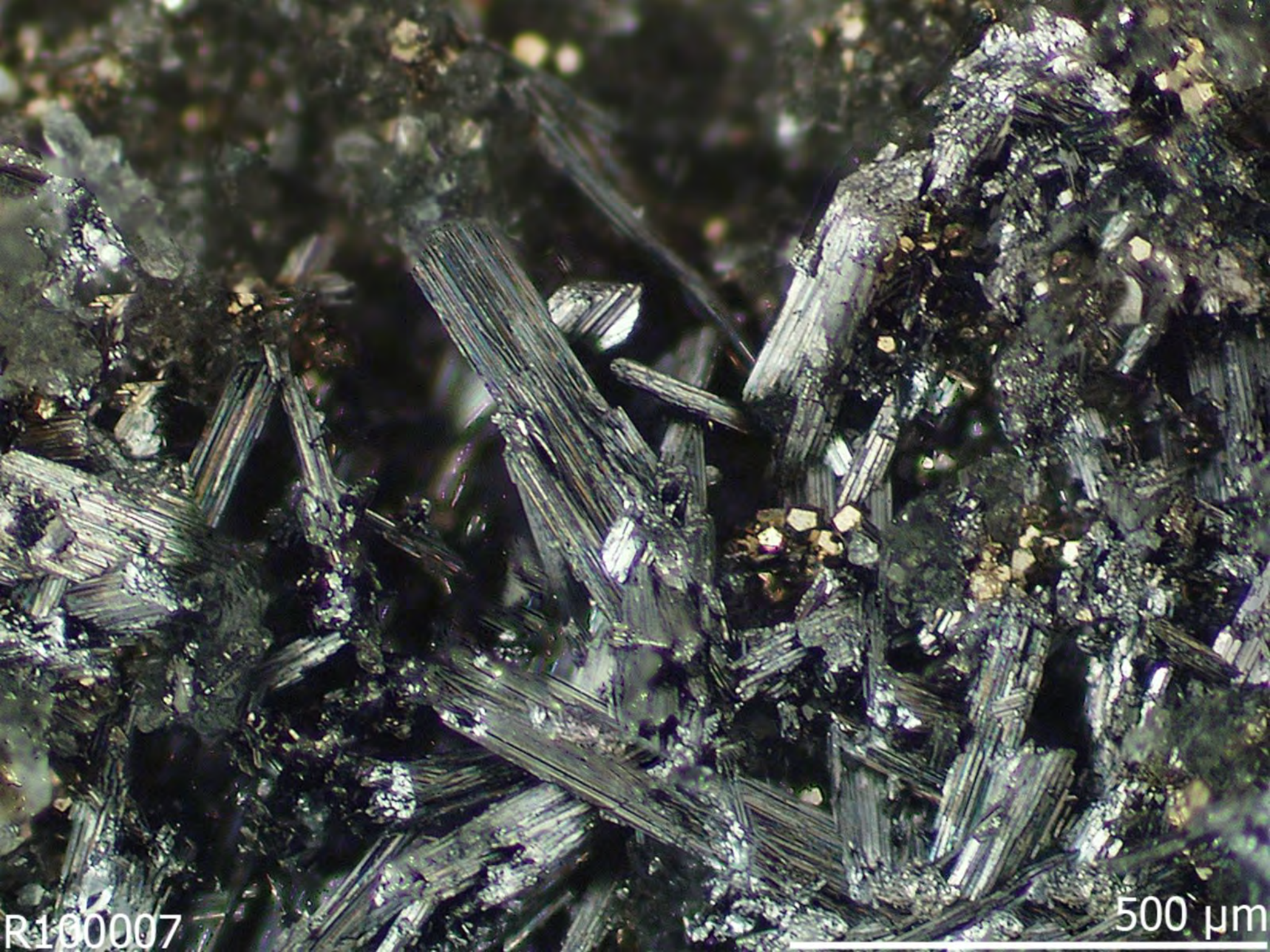
R1000007
500 µm

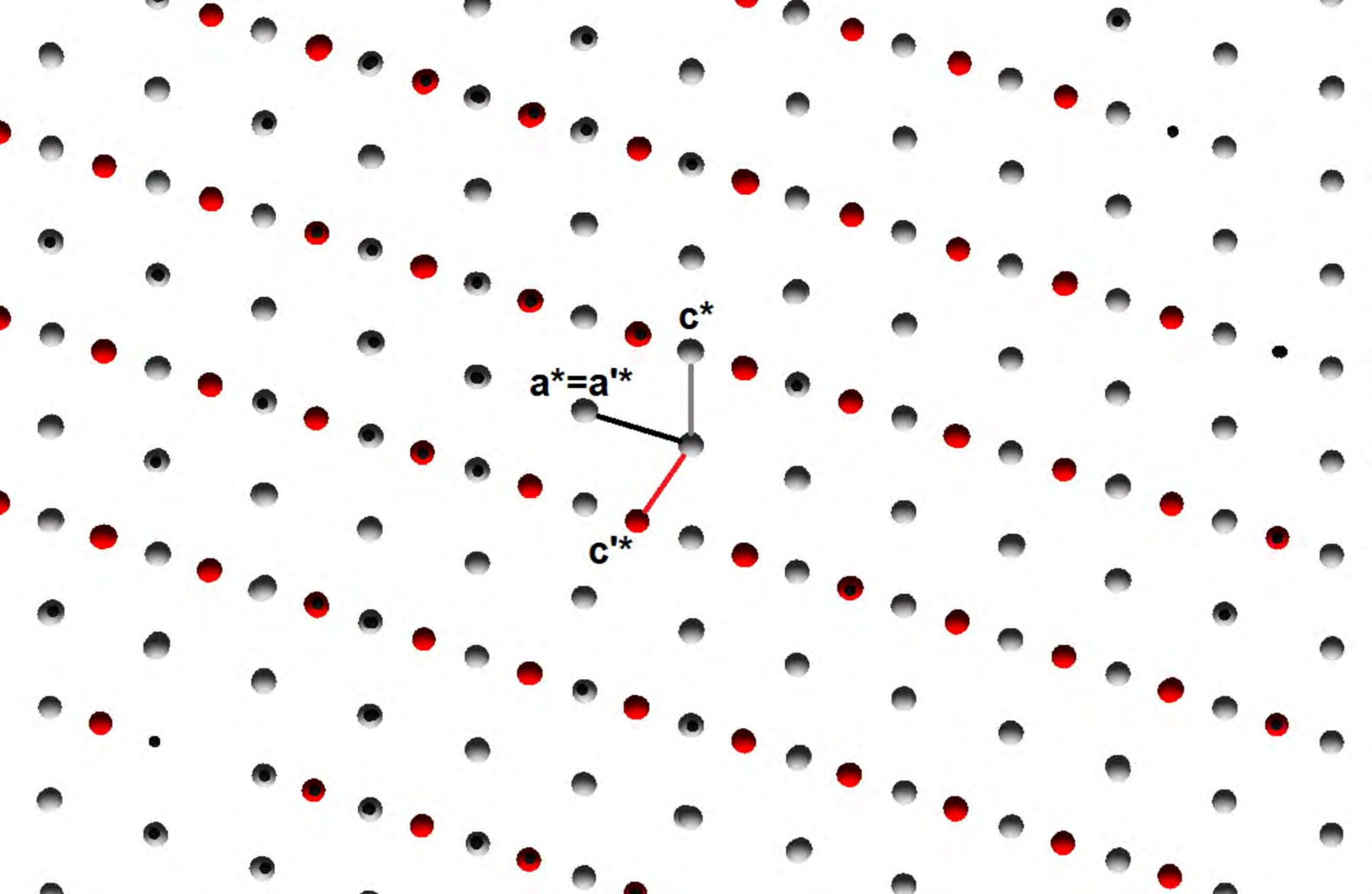
c*
a*=a'*
c'*

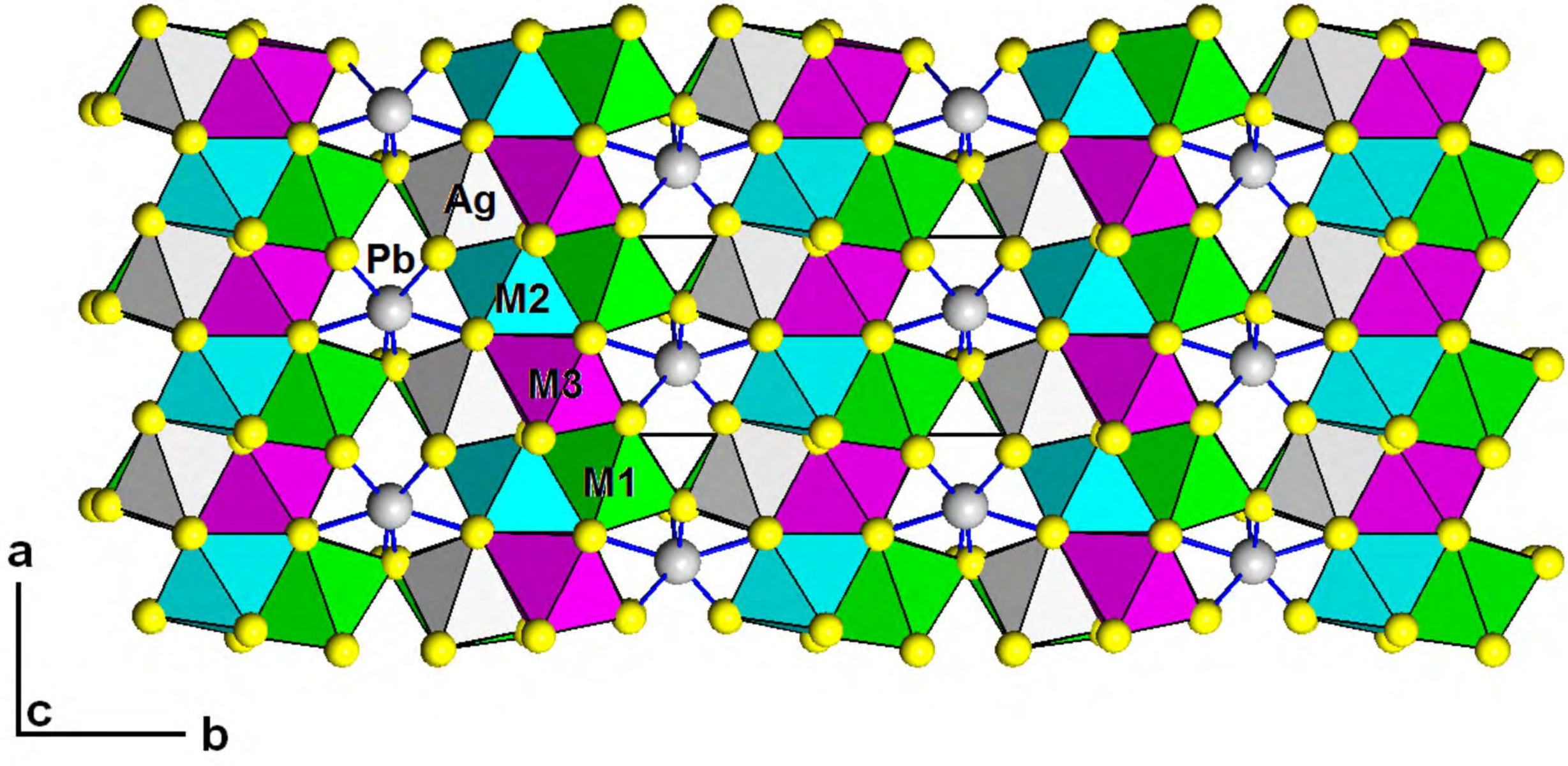
Ag
Pb
M2
M3
M1
a
c
b

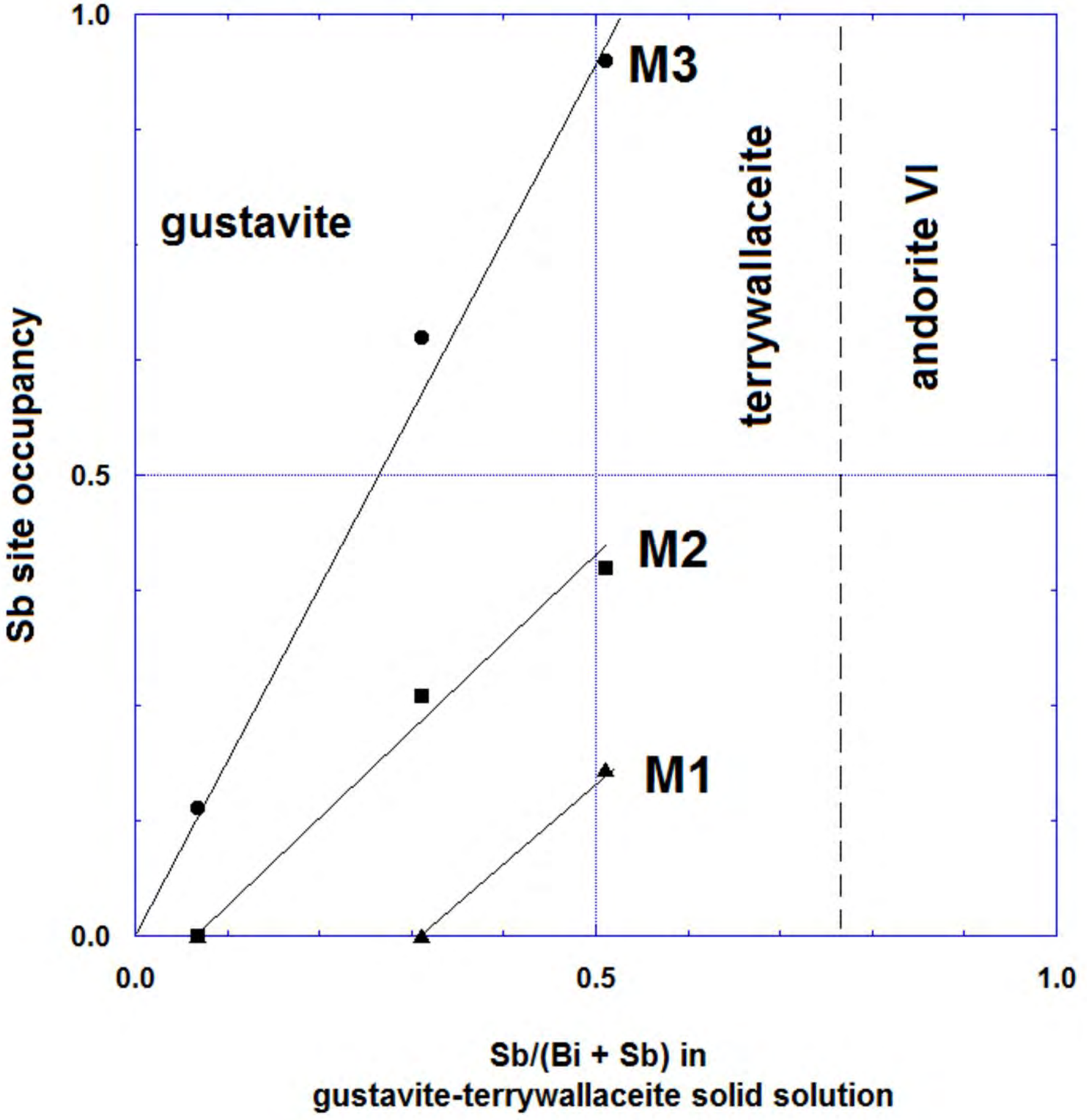
1.0
0.5
0.0
0.0
0.5
1.0
Sb site occupancy
Sb/(Bi + Sb) in
gustavite-terrywallaceite solid solution
gustavite
terrywallaceite
andorite VI
M3
M2
M1

Table 1. Reflectance values of terrywallaceite measured in air

R_{max}–R_{min}	λ
42.6–38.8	400nm
42.2–38.3	420nm
41.8–37.9	440nm
41.4–37.5	460nm
41.3–37.3	470nm
41.2–37.1	480nm
40.7–36.6	500nm
40.3–36.2	520nm
39.9–35.7	540nm
39.7–35.5	546nm
39.4–35.2	560nm
39.0–34.8	580nm
38.7–34.6	589nm
38.4–34.3	600nm
37.9–33.9	620nm
37.4–33.4	640nm
37.1–33.2	650nm
36.8–33.0	660nm
36.2–32.5	680nm
35.7–32.0	700nm

Table 2. Powder X-ray diffraction data of terrywallaceite

Experimental			Theoretical				
I_{calc}	d_{calc}(Å)		I_{calc}	d_{calc}(Å)	h	k	l
3	5.504		5	5.4819	1	2	0
4	5.025		4	5.0209	0	3	1
18	3.939		20	3.9126	1	4	0
23	**3.680**	**(2 overlaps)**	**19**	**3.6967**	**-1**	**2**	**2**
			17	**3.6958**	**0**	**2**	**2**
100	**3.369**	**(3 overlaps)**	**30**	**3.3995**	**-1**	**3**	**2**
			33	**3.3988**	**0**	**3**	**2**
			100	**3.3453**	**1**	**5**	**0**
33	**3.010**	**(2 overlaps)**	**30**	**3.0108**	**-2**	**1**	**2**
			30	**3.0093**	**1**	**1**	**2**
58	**2.911**	**(3 overlaps)**	**39**	**2.9070**	**-2**	**2**	**2**
			39	**2.9057**	**1**	**2**	**2**
			24	**2.9021**	**1**	**6**	**0**
16	2.758	**(2 overlaps)**	15	2.7557	-2	3	2
			14	2.7546	1	3	2
15	2.276	**(2 overlaps)**	11	2.2742	-1	7	2
			12	2.2740	0	7	2
12	2.126	**(3 overlaps)**	3	2.1261	2	7	0
			6	2.1223	-3	3	2
			6	2.1214	2	3	2
26	**2.080**	**(3 overlaps)**	31	2.0967	-1	0	4
			18	2.0698	-1	8	2
			17	2.0697	0	8	2
20	2.043	**(2 overlaps)**	15	2.0382	-3	4	2
			15	2.0374	2	4	2
22	1.950	**(2 overlaps)**	6	1.9435	-3	5	2
			5	1.9428	2	5	2
6	1.902	**(2 overlaps)**	7	1.8947	-2	8	2
			8	1.8943	1	8	2
7	1.852	**(3 overlaps)**	3	1.8483	-2	4	4
			5	1.8439	-3	6	2
			6	1.8433	2	6	2
17	1.771	**(2 overlaps)**	16	1.7768	-2	5	4
			16	1.7764	0	5	4
6	1.457	**(2 overlaps)**	5	1.4535	-4	4	4
			5	1.4529	2	4	4

7	1.424	9	1.4220	-1	10	4

Table 3. Summary of crystal data and refinement results for terrywallaceite and gustavite

	Terrywallaceite	Synthetic Gustavite	Sb-rich gustavite	Gustavite
Ideal chemical formula	$AgPb(Sb,Bi)_3S_6$	$AgPbBi_3S_6$	$AgPbBi_3S_6$	$AgPbBi_3S_6$
Effective structural formula	$AgPb(Sb,Bi)(Bi,Sb)_2S_6$	$(AgBi)PbBi_2S_6$	$AgPb(Sb,Bi)(Bi,Sb)_2S_6$	$Ag_{0.99}Pb(Bi_{2.90}Sb_{0.11})S_6$
Space group	$P2_1/c$ (No. 14)	*Cmcm* (No. 63)	$P2_1/c$ (No. 14)	$P2_1/c$ (No. 14)
a (Å)	6.9764(4)	4.077(2)	7.0455(6)	7.0567(14)
b (Å)	19.3507(10)	13.477(7)	19.5294(17)	19.6905(39)
c (Å)	8.3870(4)	19.88(2)	8.3412(11)	8.2219(16)
β (°)	107.519(2)	90	107.446(10)	106.961(3)
V (Å^3)	1079.7(1)	1092.3	1094.9(2)	1092.7(2)
Z	4	4	4	4
ρ_{calc} (g/cm^3)	6.005			6.789
λ (Å)	0.7107	0.7107	0.7107	0.7107
μ (mm^{-1})	32.338	67.03	54.58	63.6
2θ range for data collection	≤65.16	≤70		≤40.16
No. of reflections collected	24910		10947	6628
No. of independent reflections	3917		2408	1072
No. of reflections with $I > 2\sigma(I)$	3015	1376 [$I > 1.5\sigma(I)$]	1290 [$I > 3\sigma(I)$]	763
No. of parameters refined	106	39	103	103
R(int)	0.036		0.092	0.129
Final R_1, wR_2 factors [$I > 2\sigma(I)$]	0.034, 0.062	0.076	0.059, 0.060	0.028, 0.044
Final R_1, wR_2 factors (all data)	0.055, 0.068			
Goodness-of-fit	1.023		1.98	0.829
Twin law	(1 0 1/2, 0 -1 0, 0 0 -1)			
Twin ratio	0.74/0.26			
Reference	(1)	(2)	(3)	(4)

References: (1) this study; (2) Bente et al. (1993); (3) Pažout and Dušek (2009); (4) Makovicky and Topa (2011).

Table 4. Coordinates and displacement parameters of atoms in terrywallaceite

Atom	*x*	*y*	*z*	U_{eq}	U_{11}	U_{22}	U_{33}	U_{23}	U_{13}	U_{12}
Ag	0.13556(20)	0.36504(5)	0.28477(15)	0.0465(2)	0.0562(6)	0.0402(5)	0.0409(5)	0.0005(5)	0.0114(5)	0.0257(4)
Pb	0.63960(5)	0.25004(2)	0.15889(7)	0.0255(1)	0.0240(2)	0.0288(2)	0.0239(2)	0.0003(2)	0.0078(2)	0.0017(1)
M1	0.18850(5)	0.35966(2)	0.79992(6)	0.0164(1)	0.0153(2)	0.0171(1)	0.0171(2)	0.0005(2)	0.0053(1)	-0.0013(1)
M2	0.25787(5)	0.54936(2)	0.56150(6)	0.0164(1)	0.0176(2)	0.0144(2)	0.0169(2)	-0.0003(2)	0.0045(2)	-0.0001(1)
M3	0.72321(8)	0.44406(3)	0.92624(9)	0.0155(2)	0.0149(3)	0.0159(2)	0.0165(3)	-0.0010(2)	0.0058(3)	0.0002(2)
S1	0.0149(4)	0.4918(1)	0.2870(3)	0.0217(5)	0.0271(11)	0.0211(11)	0.0185(11)	-0.0022(8)	0.0091(9)	-0.0038(8)
S2	0.9132(3)	0.3330(1)	0.4948(3)	0.0189(4)	0.0214(9)	0.0165(9)	0.0194(11)	-0.0006(9)	0.0070(9)	-0.0007(7)
S3	0.5092(3)	0.4021(1)	0.0971(3)	0.0210(5)	0.0217(10)	0.0226(10)	0.0198(13)	-0.0023(9)	0.0078(9)	-0.0019(8)
S4	0.3547(3)	0.2390(1)	0.8390(4)	0.0190(4)	0.0184(8)	0.0199(10)	0.0184(10)	-0.0011(10)	0.0049(11)	-0.0021(7)
S5	0.5040(3)	0.5967(1)	0.3506(3)	0.0211(5)	0.0199(10)	0.0234(10)	0.0206(13)	0.0005(9)	0.0073(9)	0.0000(8)
S6	0.9209(3)	0.3351(1)	0.9730(3)	0.0188(4)	0.0206(9)	0.0159(8)	0.0206(11)	0.0018(9)	0.0073(10)	0.0027(7)

Note: M1 = 0.820(2) Bi + 0.180(2) Sb; M2 = 0.600(3) Bi + 0.400(3) Sb; M3 = 0.950(3) Sb + 0.050(3) Bi.

Table 5. Selected bond distances (Å) for terrywallaceite and gustavite.

	Terrywallaceite (1)	Sb-rich gustavite (2)	Gustavite (3)
Pb --S4	2.827(3)	2.830(5)	2.821(5)
--S4	2.843(3)	2.841(7)	2.821(4)
--S3	3.078(2)	3.101(8)	3.206(4)
--S2	3.115(2)	3.141(8)	3.220(4)
--S5	3.125(2)	3.141(8)	3.134(4)
--S6	3.224(2)	3.224(6)	3.186(5)
--S6	3.291(3)	3.311(8)	3.287(5)
--S2	3.306(2)	3.307(6)	3.283(4)
Ave.	3.101	3.112	3.120
Ag --S4	2.486(2)	2.495(8)	2.507(4)
--S1	2.595(3)	2.606(9)	2.690(4)
--S6	2.656(3)	2.708(6)	2.774(5)
--S2	2.746(3)	2.795(9)	2.731(4)
--S5	3.406(3)	3.314(6)	3.210(6)
--S3	3.501(3)	3.359(8)	3.177(4)
Ave.	2.898	2.880	2.848
M1 --S4	2.583(2)	2.609(8)	2.589(4)
--S6	2.729(2)	2.725(8)	2.720(4)
--S2	2.746(2)	2.739(6)	2.709(5)
--S3	2.922(2)	2.975(6)	3.001(5)
--S5	2.923(2)	2.980(8)	3.007(4)
--S1	3.191(2)	3.177(8)	3.132(4)
Ave.	2.849	2.868	2.860
M2 --S2	2.547(2)	2.563(8)	2.602(4)
--S1	2.658(2)	2.746(7)	2.815(4)
--S1	2.706(2)	2.776(9)	2.861(5)
--S5	2.957(2)	2.931(8)	2.879(4)
--S3	2.986(2)	2.936(6)	2.860(5)
--S5	3.248(2)	3.251(8)	3.217(4)
Ave.	2.851	2.867	2.872
M3 --S6	2.485(2)	2.540(8)	2.592(4)
--S3	2.496(2)	2.608(8)	2.675(4)
--S5	2.512(3)	2.579(6)	2.682(6)
--S1	3.169(3)	3.139(9)	3.020(5)
--S1	3.232(3)	3.159(6)	3.067(4)
--S3	3.367(2)	3.337(8)	3.281(4)
Ave.	2.877	2.894	2.886

Note: (1) This study; (2) Pažout and Dušek (2009); (3) Makovicky and Topa (2011).